Modeling and simulation of macro-crack initiation and propagation in elastic structures using a gradient-enhanced continuum damage model

S.M.P. Domingues, H.S. da Costa-Mattos
Laboratory of Theoretical and Applied Mechanics, Department of Mechanical Engineering, Universidade Federal Fluminense, Niterói/RJ – Brazil
F. A. Rochinha
Program of Mechanical Engineerin, Universidade Federal do Rio de Janeiro - COPPE/UFRJ, Rio de Janeiro/RJ – Brazil

Abstract

In order to avoid the loss of well-posedness in the post-localization range, some continuum damage theories introduce higher order gradients of the damage variable in the constitutive model. This paper discuss the possibility of structural failure prediction of quasi-brittle materials through a special kind of gradient-enhanced damage theory in which the material is considered to possess a substructure or microstructure. In these theories the microscopic movements are accounted for by the damage variable and a reformulation of the kinematics (to include the possible "micromotions") and of some basic governing principles of the classical Continuum Mechanics is necessary. The theory allows an adequate description of the strain-softening and localization behavior due to the material degradation. Within this framework, a numerically predicted macro-crack is the set of points in the structure where the damage variable has reached its critical value. A simple numerical technique, based on the finite element method, is proposed to approximate the solution of the resulting nonlinear problems. The main features of such kind of approach are discussed through examples concerning macro-crack initiation and propagation in plates under different loading conditions.

Keywords: Damage Mechanics, Finite Elements, quasi-brittle materials, crack initiation, crack propagation.

1 Introduction

Continuum Damage Mechanics uses a phenomenological approach to model the effect of microscopic geometric discontinuities induced by the deformation process (micro-cracks, micro-voids, etc.) on the macroscopic behavior of a structure. In continuum damage theories, an internal variable related to the growth and coalescence of micro defects before the macroscopic crack initiation (whose definition

Mechanics of Solids in Brazil 2009, H.S. da Costa Mattos & Marcílio Alves (Editors)
Brazilian Society of Mechanical Sciences and Engineering, ISBN 978-85-85769-43-7

and physical interpretation may vary from one model to the other) is introduced and the problem becomes to establish the constitutive relations for the damage variable as a function of the other state variables.

In the last few years, many different continuum damage theories for quasi-brittle materials have been proposed. Since the damage propagation generally leads to a local softening behaviour, the models based on a local approach, see Kachanov (1986) and Lemaitre and Chaboche [1], may lead to a physically unrealistic description of strain localization phenomena. In general, due to the loss of ellipticity of the governing equations in the post-localization range, the resulting mathematical problems may present an infinity number of solutions with discontinuous fields of displacement gradients what leads to numerical difficulties of mesh-dependence [2–5]. Some alternative approaches to the local damage theories have been proposed in the last years, see Saouridis and Mazars (1988); Bazant and Cedolin [6]; Costa-Mattos et al [7]; Frémond and Nedjar [8], Oller et al (2005), Khoei and Karimi [9], Peyrot et al [10], for example. Other approaches to the simulation of strain localization and fracture such as Ruter and Stein (2005), Carpinteri and Brighenti (2008), Brighenti [11], Lorentz [12] can be found in recent literature.

The present paper deals with an alternative theory in which the continuum is supposed to possess a substructure or microstructure. Since damage results from microscopic movements, it is proposed a reformulation of the kinematics and of some basic governing principles of the classical Continuum Mechanics in order to account for such "micro-movements". The constitutive equations are developed within a thermodynamic framework. The basic assumption is that the free energy is supposed to depend not only on the strain and the damage variable but on the damage gradient as well. Besides, to account for microscopic effects, the power of the internal forces depends not only on the velocity and its gradient, but also on the damage velocity and its gradient. The main goal is to present a numerical technique as simple as possible for approximating the resulting nonlinear mathematical problems. A splitting technique allows studying the coupled nonlinear problem through a sequence of simpler linear problems. This technique requires, at each time step, the solution of two problems: one similar to an equilibrium problem in linear elasticity and the other similar to a heat transfer problem in a rigid body.

The possibilities and main features of such kind of approach are discussed through examples concerning "crack" initiation and propagation in plates with brittle-elastic behavior under different loading conditions. The theory allows an adequate description of the strain-softening and localization behaviors due to the material degradation. The additional balance equation that governs the evolution of the damage variable prevents the occurrence of discontinuous damage gradients and, consequently, the occurrence of discontinuous displacement gradients. This fact allows an adequate simulation of severe local deformations without the numerical difficulties of mesh-dependence that arise in local continuum damage models.

2 Modeling

A body is defined as a set of material points B which occupies a region Ω of the Euclidean space at the reference configuration. In this theory, besides the classical variables that characterize the

kinematics of a continuum medium (displacements and velocities of material points), an additional scalar variable $\beta \in [0,1]$, is introduced. A point, in such continuum theory, is representative of a given "volume element" of the real material and it is endowed with a microstructure that accounts for the kinetic energy and internal power of the microscopic motions associated to the microscopic geometric discontinuities (density of micro-cracks or cavities). This variable is related with the microscopic motions or links between material points and can be interpreted as a measure of the damage state of the "volume element". If $\beta = 1$, all the links are preserved and the initial material properties are preserved. If $\beta = 0$, a local rupture is considered since all the links between material points have been broken. Since the degradation is an irreversible phenomenon, the rate $\dot{\beta}$ must be negative or equal to zero.

In the next sections the basic principles that govern the evolution of this kind of continuum are summarized. A more detailed presentation of these basic principles can be found in Costa-Mattos and Sampaio [13]. For the sake of simplicity, the hypothesis of quasi-static and isothermal processes is adopted throughout this paper. Besides, it is also assumed the hypothesis of small deformation and, consequently, the conservation of mass principle is automatically satisfied.

2.1 Principle of virtual power

In this work an arbitrary part P of the body B that occupies a region $\Omega \subset R^3$ at the reference configuration is taken as a mechanical system. By definition, the boundary of the region Ω will be called Γ. It is considered with respect to P the space V_u of all fields $\hat{\boldsymbol{u}}$ of possible velocities and the space V_β of all fields $\hat{\beta}$ of possible rates of the damage variable. V_u is called the space of virtual velocities and V_β the space of virtual damage rates.

The power of the external forces$P_{ext}(P, \hat{\boldsymbol{u}}, \hat{\beta})$, for a given virtual field of velocity $\hat{\boldsymbol{u}} \in V_u$ and for a given virtual field $\hat{\beta} \in V_\beta$ is defined as:

$$P_{ext}(P, \hat{\boldsymbol{u}}, \hat{\beta}) = P^u_{ext}(P, \hat{\boldsymbol{u}}) + P^D_{ext}(P, \hat{\beta}) \tag{1}$$

$$P^u_{ext}(P, \hat{\boldsymbol{u}}) = \int_\Omega (\boldsymbol{b} \cdot \hat{\boldsymbol{u}}) dV + \int_\Gamma (\boldsymbol{g} \cdot \hat{\boldsymbol{u}}) dA;\ P^\beta_{ext}(P, \hat{\beta}) = \int_\Omega (p\hat{\beta}) dV + \int_\Gamma (q\hat{\beta}) dA \tag{2}$$

where $(\boldsymbol{b}, \boldsymbol{g})$ are called the external forces and (p, q) the external microscopic forces. The external forces are of two kinds: contact forces $\boldsymbol{g}$ applied on the boundary Γ and volume (or body) forces $\boldsymbol{b}$ applied on Ω. Similarly, the microscopic forces are of two kinds: contact microscopic forces q applied on Γ and microscopic volume forces p applied on Ω. The power of the microscopic forces must be introduced in the theory in order to take into account the non mechanical actions that affect the cohesion state of the material even if there is no mechanical deformation.

In Continuum Mechanics it is usual to consider a first order gradient theory in which the power of the internal forces is supposed to be a function of the velocity and its gradient. In this theory, similarly as in Costa-Mattos and Sampaio [13] and Frémond, and Nedjar [8], the power of the internal forces is also supposed to be a function of β and $\boldsymbol{\nabla}\beta$. On the assumption that, for a fixed instant t, the

power of the internal forces can be expressed as a linear functional on $V_u \times V_\beta$, it may be shown that $P_{int}(P, \hat{\boldsymbol{u}}, \hat{\beta})$ must have the following form:

$$P_{int}(P, \hat{\boldsymbol{u}}, \hat{\beta}) = P^u_{int}(P, \hat{\boldsymbol{u}}) + P^\beta_{int}(P, \hat{\beta}) \tag{3}$$

$$P^u_{int}(P, \hat{\boldsymbol{u}}) = -\int_\Omega (\sigma \cdot \boldsymbol{\nabla}\hat{\mathbf{u}}) dV ; P^\beta_{int}(P, \hat{\beta}) = -\int_\Omega (\boldsymbol{H}.\boldsymbol{\nabla}\hat{\beta} + M\hat{\beta}) dV \tag{4}$$

with $\boldsymbol{\sigma}$, $\boldsymbol{H}$, M being the internal forces. $\boldsymbol{\sigma}$ is a second order tensor, $\boldsymbol{H}$ a vector and M a scalar. $\boldsymbol{\sigma}$ is the classical stress tensor and ($\boldsymbol{H}$,M) are internal microscopic forces. Similar additional internal forces also arise in classical microstructure theories such as Mindlin [14], Toupin [15], Goodman and Cowin (1972). Using the previous definitions, and assuming the hypothesis of slow deformations (hence, neglecting inertial effects) the principle of virtual power may be stated as follows:

"A given part P of B that occupies region Ω of the space at the reference configuration, is at equilibrium if the stress tensor$\boldsymbol{\sigma}$, the internal microscopic forces ($\boldsymbol{H}$,M), the external forces ($\boldsymbol{b}, \boldsymbol{g}$), the microscopic external forces (p, q) are such that

P1 - $P_{int}(P, \hat{\boldsymbol{u}}, \hat{\beta}) + P_{ext}(P, \hat{\boldsymbol{u}}, \hat{\beta}) = 0 \ \forall\ \hat{\boldsymbol{u}} \in V_u, \ \forall\ \hat{\beta} \in V_\beta$, *hence*

$$\begin{gathered} \int_\Omega [\boldsymbol{\sigma}.(\boldsymbol{\nabla}\hat{\boldsymbol{u}}) - \boldsymbol{b}.\hat{\boldsymbol{u}}]\, dV - \int_{\Gamma_2} [\boldsymbol{g}.\hat{\boldsymbol{u}}]\, dA + \int_\Omega [\boldsymbol{H} \cdot \boldsymbol{\nabla}\hat{\beta} + F\hat{\beta} - p\hat{\beta}] dV - \int_\Gamma \left[q\hat{\beta}\right] dA = 0 \\ \forall\ \hat{\boldsymbol{u}} \in V_u, \ \forall\ \hat{\beta} \in V_\beta \end{gathered} \tag{5}$$

P2 - $P_{int}(P, \hat{\boldsymbol{u}}, \hat{\beta}) = 0$ *for a rigid body motion (i.e. when $\hat{\boldsymbol{u}}(\boldsymbol{x}) = \boldsymbol{A}(\boldsymbol{x} - \boldsymbol{x_o}) + \boldsymbol{c_o}$ and $\hat{\beta}(\boldsymbol{x}) = 0$, with $\boldsymbol{x} \in \Omega$, $\boldsymbol{A}$ being an antisymmetrical tensor and $\boldsymbol{c_o}$ the velocity of a reference point $\boldsymbol{x_o} \in \Omega$)."*

Under suitable regularity assumption, it can be proved that P1 implies the following local expressions:

$$div\ \boldsymbol{\sigma} + \boldsymbol{b} = \mathbf{0} \ \ in\ \ \Omega, \ \ \boldsymbol{\sigma}.\mathbf{n} = \mathbf{f} \ \ in\ \Gamma \ \ ; \ \ div\ \mathbf{H} - M + p = 0\ in\ \Omega, \ \ \mathbf{H}.\boldsymbol{n} = q\ in\ \Gamma \tag{6}$$

where $\boldsymbol{n}$ is the unit outward normal to the surface Γ. It can also be proved that P2 implies the symmetry of the stress tensor.

2.2 Constitutive equations

Under the hypothesis of small deformations and isothermal processes, the free energy of a quasi-brittle material is supposed to be a function of the deformation ε, the damage variable β and its gradient $\boldsymbol{\nabla}\beta$. In order to resume the presentation, the thermodynamic framework used to obtain the constitutive equations is not presented in this paper. The final relations are the following:

$$\boldsymbol{\sigma} = \left(\frac{\beta \mathrm{E}}{\mathbf{1} + \nu}\right) \left[\frac{\nu}{1 - 2\nu} tr(\varepsilon)\mathbf{1} + \varepsilon\right] = \beta\, [\lambda\, tr(\varepsilon)\mathbf{1} + 2\mu\varepsilon] \tag{7}$$

$$F = \left[\frac{1}{2}\lambda\, tr(\varepsilon)^2 + \mu\, \varepsilon.\varepsilon\right] - w + \lambda_\beta + C\dot{\beta} + \lambda_{\dot{\beta}} \tag{8}$$

$$\boldsymbol{H} = k(\boldsymbol{\nabla}\beta) \tag{9}$$

Where E is the Young modulus, ν is the Poisson's ratio, λ and μ are the Lamé constants. The terms λ_β and $\lambda_{\dot\beta}$ are Lagrange multipliers associated, respectively, to the constraints $\beta \geq 0$ and $\dot\beta \leq 0$, they are such that: $\lambda_\beta \leq 0$, $\beta\,\lambda_\beta = 0$ and $\lambda_{\dot\beta} \leq 0$, $\dot\beta\,\lambda_{\dot\beta} = 0$.

2.3 Mechanical problem

Neglecting the external microscopic forces p and q, the following integral formulation for the quasi-static evolution problem can be obtained introducing constitutive equations (7) - (9) in (5)

"Let a body B that occupies a region $\Omega \subset R^3$ with a sufficiently regular boundary Γ be subjected at each time instant t to external forces – a contact force $\boldsymbol{g} \;:\; \Gamma_2 \subset \Gamma \rightarrow R^3$, and a body force $\boldsymbol{b}(t) \;:\; \Omega \rightarrow R^3$ – and to prescribed displacements $\bar{\boldsymbol{u}}(t)$ and damage fields $\bar\beta(t)$ in $\Gamma_1 \subset \Gamma$, where $\Gamma = \Gamma_1 \cup \Gamma_2$ and $\Gamma_1 \cap \Gamma_2 = \varnothing$. Find the displacement field $\boldsymbol{u}(t) \;:\; \Omega \rightarrow R^3$ with $\boldsymbol{u}(t)|_{\Gamma_1} = \bar{\boldsymbol{u}}(t)$ and the field $\beta(\boldsymbol{x},t) \;:\; \Omega \rightarrow R$ with $\beta(t)|_{\Gamma_1} = \bar\beta(t)$, such that, for all time instant $t \in [0,\tau]$

$$\begin{array}{c} a_\varepsilon(\boldsymbol{u},\hat{\boldsymbol{u}},\beta) - l_\varepsilon(\hat{\boldsymbol{u}}) = 0 \\ a_\beta(\beta,\hat\beta) + l_\beta(\boldsymbol{u},\hat\beta) + \mathrm{c}_\beta(\dot\beta,\hat\beta) + \Lambda_\beta(\beta,\hat\beta) + \Lambda_{\dot\beta}(\dot\beta,\hat\beta) = 0 \end{array} \qquad \forall\ \hat u \in V_u,\ \forall\ \hat\beta \in V_\beta \tag{10}$$

with the initial condition $\beta(t=0) = 1$ and subjected to the constraints: $\dot\beta \leq 0$, $\beta \geq 0$"

a_ε, l_ε, a_β, l_β and c_β are defined as follows:

$$a_\varepsilon(\boldsymbol{u},\hat{\boldsymbol{u}},\beta) = \int_\Omega \beta[\lambda\, div\boldsymbol{u}\; div\hat{\boldsymbol{u}} + 2\mu\; \boldsymbol{\nabla u}.\boldsymbol{\nabla}\hat{\mathbf{u}}]dV \tag{11}$$

$$l_\varepsilon(\hat{\boldsymbol{u}}) = \int_\Omega [\boldsymbol{b}.\hat{\boldsymbol{u}}]\, dV + \int_{\Gamma_2} [\boldsymbol{g}.\hat{\boldsymbol{u}}]\, dA \tag{12}$$

$$a_\beta(\beta,\hat\beta) = \int_\Omega \left[k\nabla\beta.\nabla\hat\beta\right] dV \tag{13}$$

$$l_\beta(\hat\beta,\boldsymbol{u}) = \int_\Omega \hat\beta\, [\frac{1}{2}\lambda\, (div\boldsymbol{u})^2 + \mu\; \boldsymbol{\nabla u}.\boldsymbol{\nabla u} - w + \lambda_\beta + \lambda_{\dot\beta}]dV \tag{14}$$

$$c_\beta(\hat\beta,\dot\beta) = \int_\Omega \left[C\dot\beta\hat\beta\right] dV \tag{15}$$

$$\Lambda_\beta(\hat\beta,\beta) = \int_\Omega \left[\lambda_\beta\hat\beta\right]\; dV;\;\; \lambda_\beta \leq 0,\; \beta\lambda_\beta = 0 \tag{16}$$

$$\Lambda_{\dot\beta}(\hat\beta,\dot\beta) = \int_\Omega \left[\lambda_{\dot\beta}\hat\beta\right]\; dV;\;\; \lambda_{\dot\beta} \leq 0,\; \dot\beta\lambda_{\dot\beta} = 0 \tag{17}$$

3 Numerical approximation of the integral problem

The abstract mathematical problem (10) is similar to the one that arises in the study of heat transfer in elastic bodies undergoing small transformations. Hence, numerical strategies adopted for the solution of coupled heat transfer problems can be easily adapted to this case [16, 17]. This coupled nonlinear problem can be solved through a strategy in which the semi-discrete problem that results from a spatial discretization is splitted in a sequence of two linear systems of ordinary differential equations, which are in turn solved by standard time integration techniques. Such a staggered scheme can be viewed as a product formula algorithm, exactly as in the classical method of fractional steps [18, 19].

3.1 Semi-discrete problem

The solution of the damage evolution problem is based on a spatial discretization leading to a semi-discrete version (a nonlinear system of ordinary differential equations). This system of differential equations is approximated through a sequence of two linear problems, which are in turn solved by standard time integration techniques. Let's consider V_u^m a m-dimensional sub-space of the space V_u, generated by a finite set of base functions $\boldsymbol{N}_i (1 = 1, \ldots, m)$ and V_β^m a n-dimensional subspace of the space V_β, generated by a finite set of base functions $\varphi_i (1 = 1, \ldots, n)$. These base functions allow the construction the approximations $\boldsymbol{u}_m$ and β_n for $\boldsymbol{u}$ and β:

$$\boldsymbol{u}_m(\boldsymbol{x}, t) = \sum_{i=1}^{m} (w_i(t)\boldsymbol{N}_i(\boldsymbol{x})) + \bar{\boldsymbol{u}}(t) \text{ and } \beta_n(\boldsymbol{x}, t) = \sum_{i=1}^{n} (\zeta_i(t)\varphi_i(\boldsymbol{x})) + \bar{\beta}(t) \tag{18}$$

Where $\bar{\boldsymbol{u}}(t)$ and $\bar{\beta}(t)$ are given functions satisfying the boundary conditions imposed in Γ_1. The spaces V_u^m and V_β^n may have different dimension ($m \neq n$). Nevertheless, to simplify the presentation, from now on, both spaces are supposed to have the same dimension ($m = n$). The semi-discrete problem is obtained by replacing $\boldsymbol{u}$ by $\boldsymbol{u}_m$ and β by β_m in the governing equations presented in (10). It can be verified that the resulting semi-discrete problem is a nonlinear system of first order ordinary differential equation with the following form:

$$[\mathbf{K}(\boldsymbol{\beta})]\,\mathbf{U} = \mathbf{R};\ [\mathbf{C}]\,\dot{\boldsymbol{\beta}} + [\mathbf{A}]\,\boldsymbol{\beta} + [\mathbf{F}(\mathbf{U})] + \left[\boldsymbol{\Upsilon}_\beta(\dot{\boldsymbol{\beta}})\right] + \left[\boldsymbol{\Upsilon}_{\dot{\beta}}(\dot{\boldsymbol{\beta}})\right] = \mathbf{0} \tag{19}$$

where

$$\left.\begin{array}{c} \mathbf{U} = \{w_1, w_2, ..., w_m\}\ ;\ \boldsymbol{\beta} = \{\zeta_1, \zeta_2, ..., \zeta_m\}\ ;\ \dot{\boldsymbol{\beta}} = \left\{\dot{\zeta}_1, \dot{\zeta}_2, ..., \dot{\zeta}_m\right\} \\ [\mathbf{K}(\boldsymbol{\beta})]_{ij} = a_\varepsilon(\mathbf{N}_i, \mathbf{N}_j, \beta_m)\ ;\ [\mathbf{C}]_{ij} = c_\beta(\varphi_i, \varphi_j)\ ;\ [\mathbf{A}]_{ij} = a_\beta(\varphi_i, \varphi_j) \\ [\mathbf{R}]_i = \mathbf{l}_\varepsilon(\mathbf{N}_i)\ ;\ \ [\boldsymbol{F}(\boldsymbol{U})]_i = l_\beta(\varphi_i, \boldsymbol{u}_m) \\ \left[\boldsymbol{\Upsilon}_{\boldsymbol{\beta}}(\dot{\boldsymbol{\beta}})\right]_i = \Lambda_\beta(\varphi_i, \beta_m)\ \ ;\ \left[\boldsymbol{\Upsilon}_{\dot{\boldsymbol{\beta}}}(\dot{\boldsymbol{\beta}})\right]_i = \Lambda_{\dot{\beta}}(\varphi_i, \dot{\beta}_m), \quad i, j = 1, ..., m \end{array}\right\} \tag{20}$$

If the base function are chosen following the classical Finite Element technique, the parameters w_i (i=1,...,m) at a given instant t can be associated to the components of the displacement $\boldsymbol{u}$ at the nodal points and the parameters ζ_i (i=1,...,m) to the value of the auxiliary variable β at the

nodal points. From now on, it is supposed that the Finite Element technique is adopted and that the parameters w_i and ζ_i can have such physical interpretation. Nevertheless, the notation will be kept intentionally general and abstract, since any adequate choice of base functions (such as in the element-free Galerkin method [20]) can also be adopted alternatively in the semi-discretization.

3.2 Operator splitting technique applied to semi-discrete problem

A splitting Technique is used to approximate the nonlinear semi-discrete problem through a sequence of simpler linear problems. In the following, it is considered a time step Δt and the notation: $t_n = (n\ \Delta t)$ and $y(t_n) = y^n$. If all the fields are known at a given instant t_n, the nodal variables β^{n+1} and $\mathbf{U}^{n+1}$ can be approximated by solving the following sequence of linear problems

i) β^{n+1} is the solution of

$$[\mathbf{C}]\left\{\theta\boldsymbol{\beta}^{n+1} + (1-\theta)\boldsymbol{\beta}^{n}\right\} + \Delta t\,[\mathbf{A}]\left\{\theta\boldsymbol{\beta}^{n+1} + (1-\theta)\boldsymbol{\beta}^{n}\right\} + \Delta t\,[\mathbf{F}(\mathbf{U}^{n})] = \mathbf{0}$$

ii) Projection 1: if $\beta_i^{n+1} \geq \beta_i^n \rightarrow \beta_i^{n+1} = \beta_i^n;\ \ i = 1, \ldots, m$

iii) Projection 2: if $\beta_i^{n+1} < \delta \Rightarrow \beta_i^{n+1} = \beta_i^n$

iv) $\mathbf{U}^{n+1}$ is the solution of $\left[\mathbf{K}(\boldsymbol{\beta}^{n+1})\right]\ \boldsymbol{U}^{n+1} = \boldsymbol{R}^{n+1}$

Projection technique adopted in step (ii) aims to assure that the constraint $\dot{\beta} \leq 0$ is verified in all nodal points. Projection technique adopted in step (iii) assures that $\beta \geq 0$ in all nodal points. $\delta > 0$ is the smallest admissible numerical value of the damage variable β. The choice of δ depends on the precision of the machine, but it is suggested $10^{-6} \leq \delta \leq 10^{-5}$. θ defines the integration method: $\theta = 0$, forward Euler; $\theta = 1$, backward Euler and $\theta = 1/2$, trapezoidal rule. A similar procedure to approximate $\boldsymbol{\beta}^{n+1}$ and $\mathbf{U}^{n+1}$ can be considered using a different sequence of linear problems:

i) $\mathbf{U}^{n+1}$ is the solution of $[\mathbf{K}(\boldsymbol{\beta}^{n})]\ \boldsymbol{U}^{n+1} = \boldsymbol{R}^{n+1}$

ii) $\boldsymbol{\beta}^{n+1}$ is the solution of $[\mathbf{C}]\left\{\theta\boldsymbol{\beta}^{n+1} + (1-\theta)\boldsymbol{\beta}^{n}\right\} + \Delta t\,[\mathbf{A}]\left\{\theta\boldsymbol{\beta}^{n+1} + (1-\theta)\boldsymbol{\beta}^{n}\right\} +$
$$+\Delta t\left\{\theta\,[\mathbf{F}(\mathbf{U}^{n})] + (1-\theta)\left[F(U^{n+1})\right]\right\} = \mathbf{0}$$

iii) Projection 1: if $\beta_i^{n+1} \geq \beta_i^n \rightarrow \beta_i^{n+1} = \beta_i^n;\ \ i = 1, \ldots, m$

iv) Projection 2: if $\beta_i^{n+1} < \delta \Rightarrow \beta_i^{n+1} = \beta_i^n$

A reasonable criterion to verify if the approximation of a given problem is adequate is to compare the different solutions obtained using these two different procedures. Generally they are very close, even if sufficiently small time interval is considered.

4 Results and discussion

A local governing equation for the damage variable β can be obtained introducing (8), (9) into the second expression in (6):

$$C\dot{\beta} = k\ \Delta\beta + w - \left[\frac{1}{2}\lambda\ tr(\varepsilon)^2 + \mu\ \varepsilon.\varepsilon\right] - \lambda_\beta - \lambda_{\dot{\beta}} \tag{21}$$

Eq. (21) is similar to the heat transfer equation for elastic bodies undergoing small transformations. Parameter C plays the same role than the specific heat (the smaller is C the bigger is the damage variation for a given supply of mechanical power). k has a similar role than the thermal conductivity (the smaller is k, the more localized is the damage). The main difference is the limit defined by parameter w – at a given material point, $\dot{\beta} \neq 0$ only if $\left[\frac{1}{2}\lambda\, tr(\varepsilon)^2 + \mu\, \varepsilon.\varepsilon\right] > w$. Hence, it is necessary a minimum strain energy w in order to have a local evolution of the damage variable.

As a first step to assess the main features of the modeling, a one-dimensional problem is considered in the next section. The main goal is to study the influence of the material parameters on the material behavior through a simple example. The features of the numerical solution strategy are discussed in three other examples concerning the crack initiation and propagation in plates under different conditions.

4.1 A non-homogeneous one-dimensional problem

In this first example, it is considered a bar of length L, submitted to the following boundary conditions

$$u_x(x=0,t)=0, u_x(x=L,t)=\alpha t \text{ and } \beta(x=0,t)=1, \beta(x=L,t)=1, \forall t \tag{22}$$

Neglecting the weight of the bar ($\boldsymbol{b}=\mathbf{0}$) and assuming it is not submitted to external microscopic forces ($p=q=0$), the local governing equations can be expressed as follows in a one-dimensional context

$$\frac{\partial \sigma_{xx}}{\partial x} = 0 \tag{23a}$$

$$\frac{\partial u_x}{\partial x} = \frac{\sigma_{xx}}{E\beta} \tag{23b}$$

$$\frac{\partial \beta}{\partial t} = \begin{cases} -\frac{1}{C}\left\langle \frac{1}{2E}\left(\frac{\sigma_{xx}}{\beta}\right)^2 - w - k\frac{\partial^2 \beta}{\partial x^2}\right\rangle, \text{ if } 0<\beta\leq 1 \\ 0, \text{ if } \beta = 0 \end{cases} \tag{23c}$$

Defining the dimensionless variables $(\sigma^*, x^*, u^*, t^*)$ and the dimensionless quantities (C_1, C_2):

$$\sigma^* = \frac{\sigma_{xx}}{E}, x^* = \frac{x}{L} u^* = \frac{u_x}{L}, t^* = \frac{E}{C}t, C_1 = \frac{w}{E}, C_2 = \frac{k}{L^2 E} \tag{24}$$

problem (22), (23) can be re-written as follows:

$$\frac{\partial \sigma^*}{\partial x^*} = 0 \tag{25a}$$

$$\frac{\partial u^*}{\partial x^*} = \frac{\sigma^*}{\beta} \tag{25b}$$

$$\frac{\partial \beta}{\partial t^*} = \begin{cases} -\left\langle \frac{1}{2}\left(\frac{\sigma^*}{\beta}\right)^2 - C_1 - C_2\frac{\partial^2 \beta}{\partial (x^*)^2}\right\rangle, \text{ if } 0<\beta\leq 1 \\ 0, \text{ if } \beta = 0 \end{cases} \tag{25c}$$

with

$$\begin{aligned} &u^*(x^*=0,t^*)=0,\ u^*(x^*=1,t^*)=\hat{\alpha}t^*=\left(\tfrac{\alpha C}{EL}\right)t^* \\ &\beta(x^*=0,t^*)=1,\ \beta(x^*=1,t^*)=1 \end{aligned} \qquad \forall t \tag{26}$$

This simple one-dimensional example shows that the model accounts for the size effect through the parameter C_2 (the behavior of the structure will depend on the length L). Although the (dimensionless) axial stress component σ^* is constant along the bar, it will undergo a non homogeneous deformation due to the damage. Fig. 1 shows the distribution of the axial strain component $\varepsilon = \frac{\partial u^*}{\partial x^*}$ at instant $t^* = 3.555 \times 10^5$ for two different values of the parameter C_2 considering $C_1 = 5 \times 10^{-7}$ and $\hat{\alpha} = 10^{-8}$. It can be observed that the smaller is C_2 (or k), the more localized is the deformation at the middle of the bar.

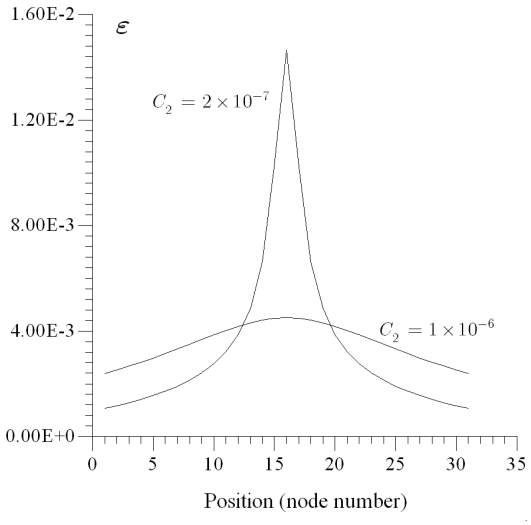

Figure 1: Distribution of the axial deformation along the bar for two different values of C_2.

Fig. 2 shows the influence of the parameter C_2 on the (dimensionless) axial stress versus axial strain curve at the point $x^* = 1/2$, taking $C_1 = 5 \times 10^{-7}$ and $\hat{\alpha} = 10^{-8}$. Parameter w (or the dimensionless parameter C_1) is related to the minimum strain energy necessary to start the damage evolution at a given point. In the one-dimensional case it corresponds to the area of the linear portion of the stress-strain curve, see Fig 3.

Parameter C (or the dimensionless parameter $\hat{\alpha}$) has a similar role than the specific heat in a one dimensional heat transfer problem in an elastic bar. Fig. 4 shows the (dimensionless) axial stress versus axial strain curve at the point $x^* = 1/2$, taking $C_2 = 2 \times 10^{-7}$, $C_1 = 5 \times 10^{-7}$ and different values of $\hat{\alpha}$.

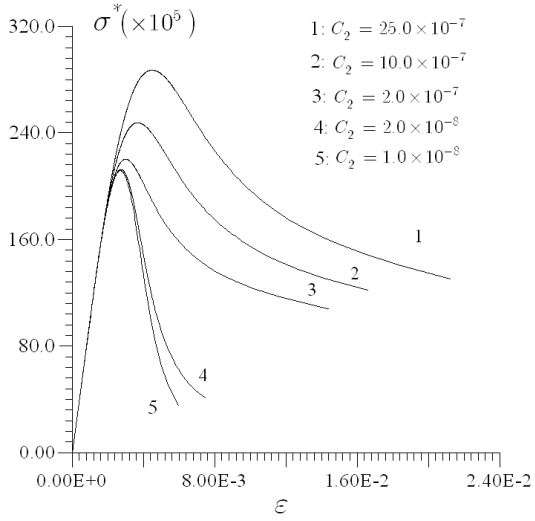

Figure 2: Influence of the parameters C_2 on the structure behavior.

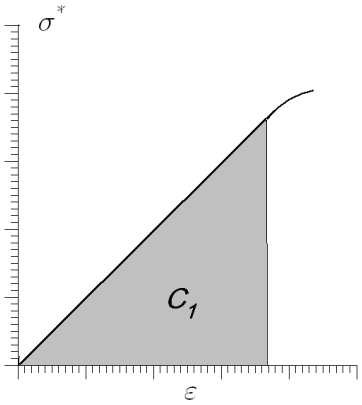

Figure 3: Definition of the parameter C_1.

4.2 Square plate with transverse hole submitted to prescribed axial displacement

In order to assess the features of the modeling, it is analyzed a square plate (200 mm x 200 mm) with a central circular hole with 50 mm radius, submitted to prescribed displacement $\hat{u}(t) = \alpha t$, $\alpha = 2.5\times10^{-3}\ mm/s$, at the extremities (Fig. 5). The goal is to study the "crack" initiation on such kind of structure. The material properties are: E=27.0GPa, $\nu = 0.2$, $k = 0.2$ MPa.mm^2, $C = 1.0\times10^{-8}$ MPa.s and $w = 5.0\times10^{-8}$ MPa. The prescribed displacement and the adopted time step are respectively

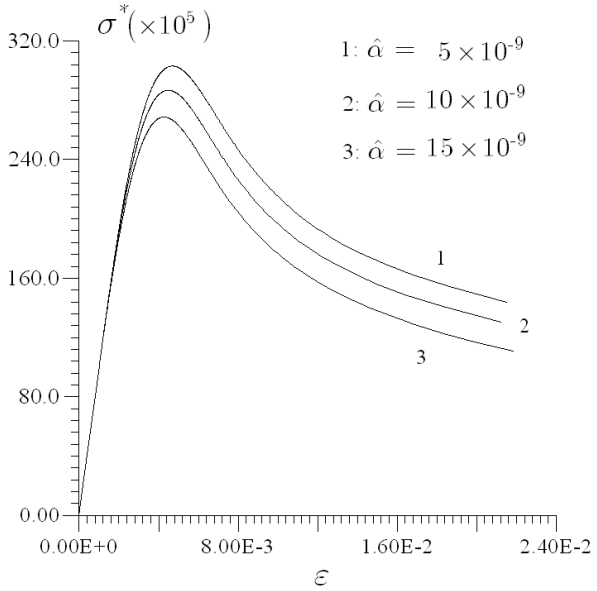

Figure 4: Influence of the parameters $\hat{\alpha}$ on the structure behavior.

given by $u(L,t) = \alpha t$, ($\alpha = 5.0 \times 10^{-3}\ mm/s$). Plane state of strain is assumed and isoparametric bi-linear quadrilateral finite elements are adopted with time step $\Delta t = 1.0 \times 10^{-4}\ s$.

The evolution of the variable $D = (1-\beta)$ on the plate is depicted in Fig. 6. Considering a numerically predicted macro-crack the set of points in the structure where the damage variable has reached a given critical value, it can be observed a straight "macro-crack" initiation and propagation orthogonally to the load direction. The region where the material is completely damaged ($\beta = 0$ or, equivalently, $D = 1$) is not limited to a column of elements as it happens in a mesh dependent problem.

Fig. 7 presents the damage and axial stress fields at instant t = 3.0 s. In this theory, the stress at the tip of the "crack" is zero (since $\beta = 0$) and the higher stress concentration (but with a finite value) occurs a little ahead of the "crack" tip.

Fig. 8 shows the distribution of the longitudinal displacement along the plate at three different time steps. As it can be verified, after instant t=3.35 s, total failure occurs and the "broken" part of the plate almost undergoes a rigid body motion.

The external tensile force F versus prescribed displacement $\hat{h}$ curves for the four different meshes in Fig. 10 are presented in Fig. 9. The softening behavior is almost the same for all the meshes showing that numerical difficulties of mesh-dependence due to the loss of ellipticity of the governing equations in the post-localization range are not observed in this case.

Fig. 12 allows to observe the damage propagation along the horizontal lines A (y = 53.0 mm) and B (y = 60.0 mm), defined in Fig 11. The shapes of the curves and the damage levels at different points along those lines are almost the same for different meshes.

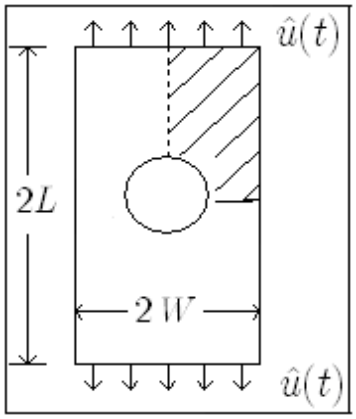

Figure 5: Plate with central circular hole.

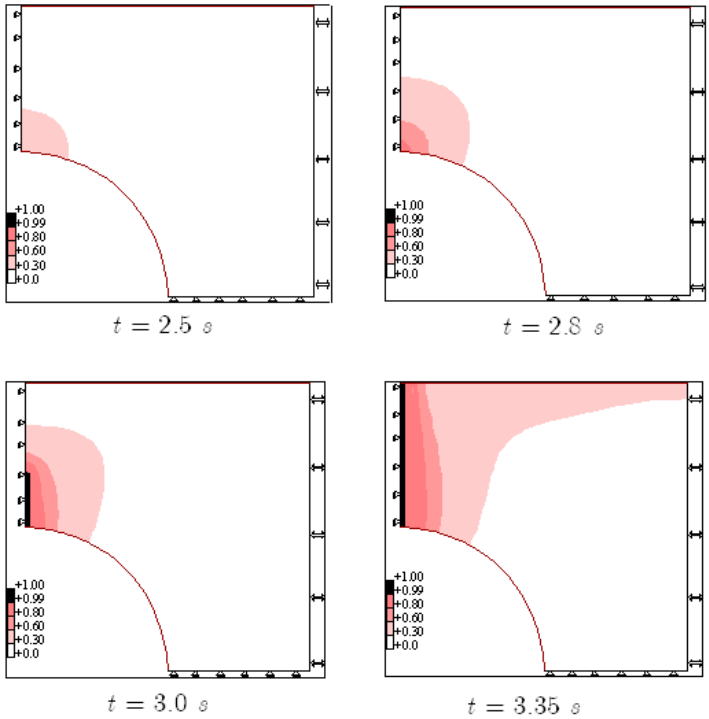

Figure 6: Plate with central circular hole. Damage distribution at different instants.

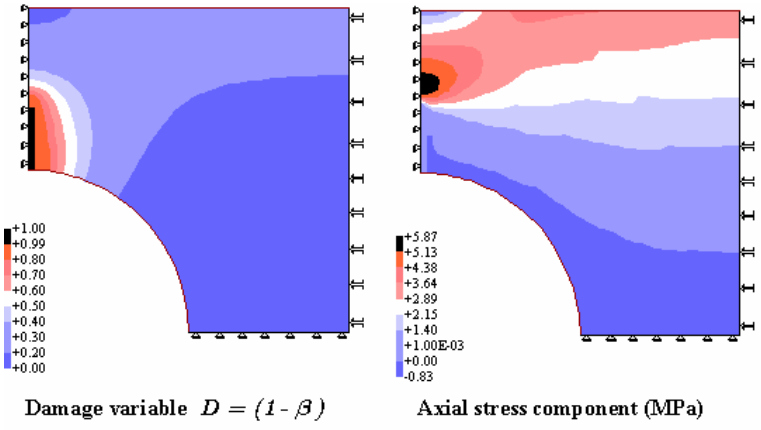

Figure 7: Plate with central circular hole. Damage and axial stress distribution. $t = 3.0\ s$.

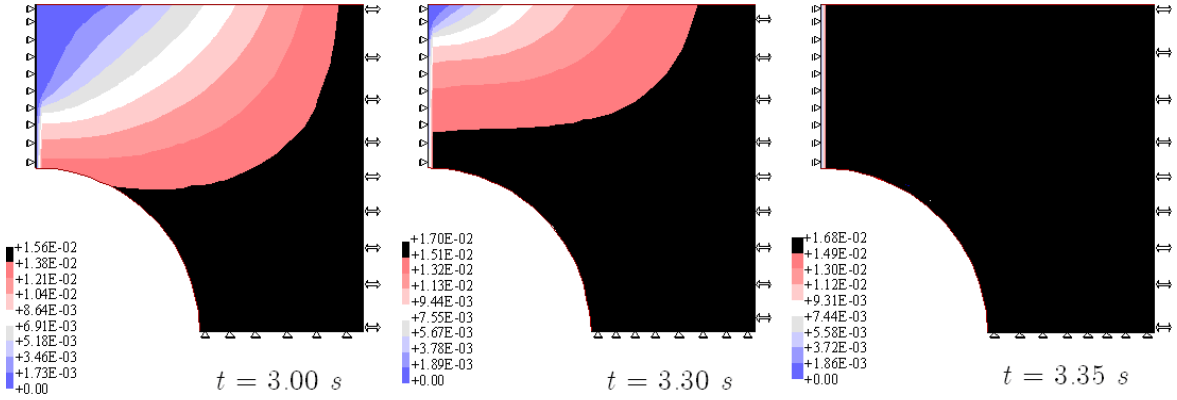

Figure 8: Plate with central circular hole. Distribution of the longitudinal displacement along the plate at three different time steps.

The performance of the proposed algorithm is also checked by comparing the distribution of variable β and longitudinal displacement u obtained using different time steps Δt and the same spatial discretization, mesh-2 (Fig. 9). Backward Euler ($\theta = 1$) time integration scheme was employed. The time increments considered in the simulations are 0.1 s, 0.01 s, 0.001 s, 0.0005 s and 0.0001 s. The distribution of the variables β and u along the line B, at instant $t =$ 3.0s, is presented in Fig 13. The curves obtained using time increments Δt=0.0005s and Δt=0.0001s are indiscernible within the precision of the figure.

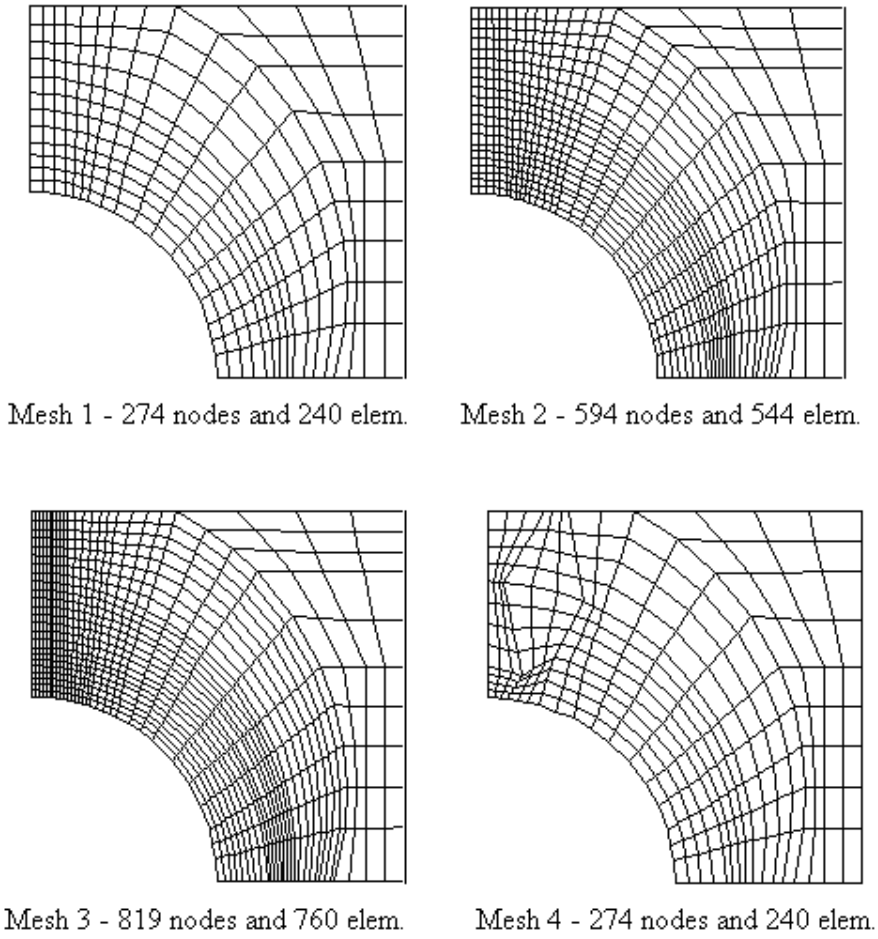

Figure 9: Plate with central circular hole. Analysis of mesh dependence - Different meshes considered.

4.3 Double-edge-cracked plate submitted to a prescribed axial displacement

It is considered in this section a double-edge-cracked plate (25 mm x 10 mm), with initial crack length of 4 mm, loaded with a prescribed displacement $\hat{u}(t) = \alpha t$, $\alpha = 5.0 \times 10^{-3}\ mm/s$, at both sides (Fig. 14). In this case, the goal is to perform the analysis of a "crack" propagation. The material properties are the same than the previous example. Plane state of strain is assumed and isoparametric bilinear quadrilateral finite elements are used with a time step $\Delta t = 1.0 \times 10^{-4}$.

Fig. 15 shows the damage field $D = (1 - \beta)$ on the plate at three different time steps. Fig. 16 shows the longitudinal displacement along the plate. As it can be verified, after instant t=1.577s, total failure occurs and the "broken" part of the plate undergoes a rigid body motion.

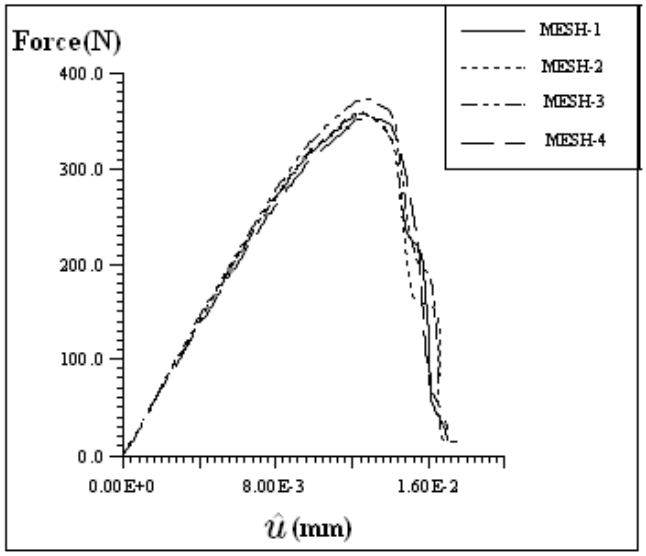

Figure 10: Plate with central circular hole. Tensile force versus displacement $\hat{u}$.

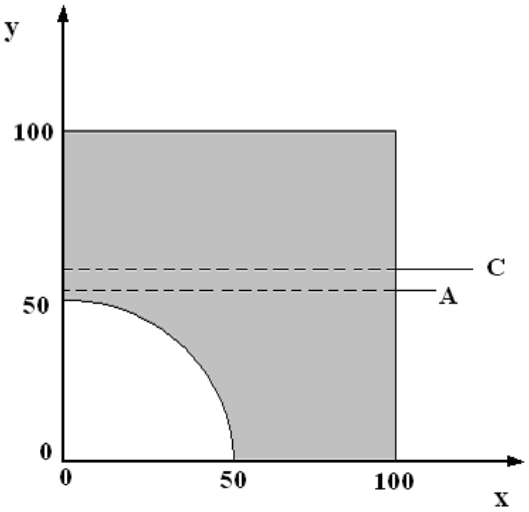

Figure 11: Plate with central circular hole. Longitudinal lines A and B.

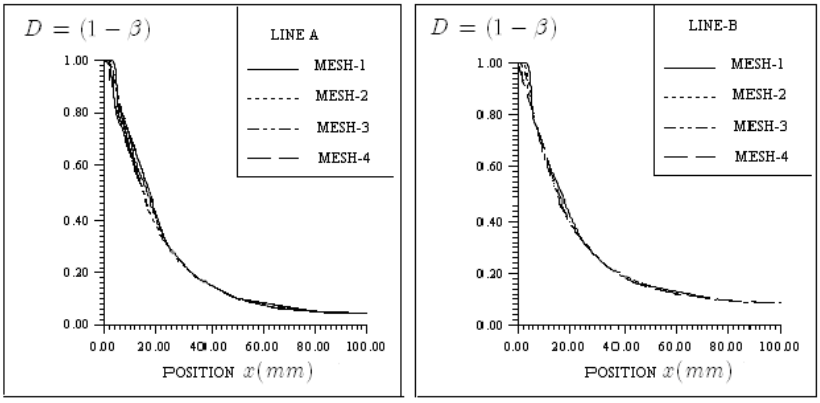

Figure 12: Plate with central circular hole. Damage along lines A and B.

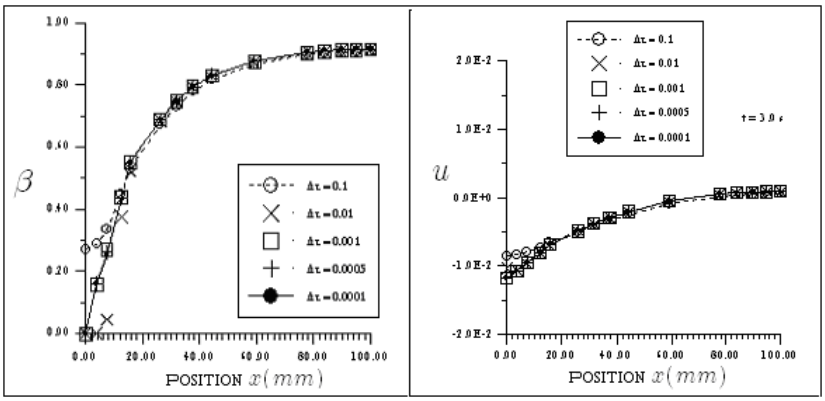

Figure 13: Plate with central circular hole. Distribution of variables β and u along the line along line B, at t = 3.0s

The external tensile force F versus prescribed displacement $\hat{u}$ curves for the three different meshes in Fig. 17 are presented in Fig. 18. Mesh-1 has 340 nodes and 304 elements, mesh-2 has 500 nodes and 456 elements and mesh-5 has 252 nodes and 221 elements. Mesh 3 is deliberately distorted to check the sensitivity of the numerical solution to the choice of the mesh. The softening behavior is almost the same for all the meshes showing that numerical difficulties of mesh-dependence are not observed in this case.

Fig. 19 shows the damage distribution at instant t_f when total failure occurs for the 3 different meshes. The damage distribution is practically the same for all the meshes.

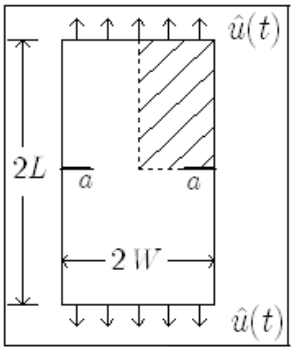

Figure 14: Double-edge-cracked plate.

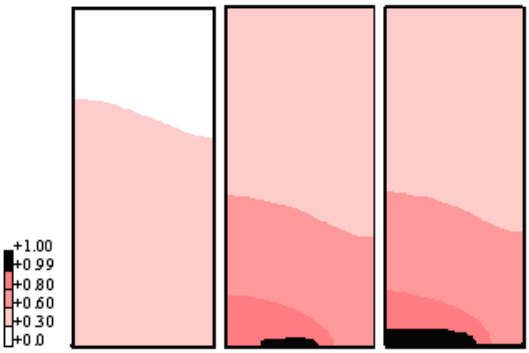

Figure 15: Double-edge-cracked plate. Damage distribution at instants t = 1.3 sec, t = 1.575 sec and t =1.577sec.

4.4 Rectangular plate, clamped at the ends and submitted to a prescribed axial displacement

It is considered in this section a rectangular plate (200mm x 100 mm) clamped at the ends and submitted to a prescribed axial displacement $\hat{u}(t) = \alpha t$, $\alpha = 1.0\text{x}10^{-2} mm/s$, at the extremities (Fig. 20). The material parameters are: E=50.0GPa, ν=0.2, $C = 1.0 \times 10^{-3}$ MPa.s and $w = 2.5 \times 10^{-2}$ MPa. In this case, the goal is to perform the analysis of a "crack" initiation and propagation in a complex mode.

Fig 21 shows the vertical displacement along the plate at the moment total failure occurs, considering two different values of the parameter k: 1 MPa.mm^2 (t=30 s) and 0.5 MPa.mm^2 (t = 24 s). Initially a "macro-crack" appears on the left corner at the bottom of the plate initially propagates orthogonally to the load direction and then changes the direction of propagation until total failure occurs (with two regions almost undergoing a rigid body motion). The "macro-crack" can be associated to the zone of

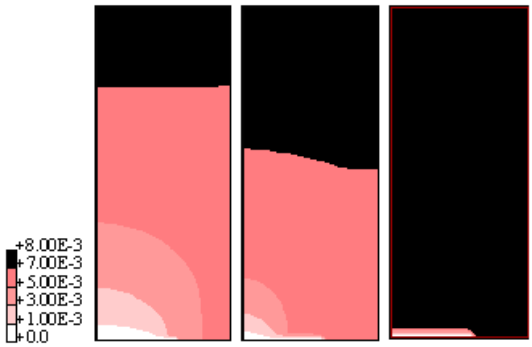

Figure 16: Double-edge-cracked plate. Longitudinal displacement (mm) at instants t = 1.3 s, t = 1.575 s and t = 1.577s.

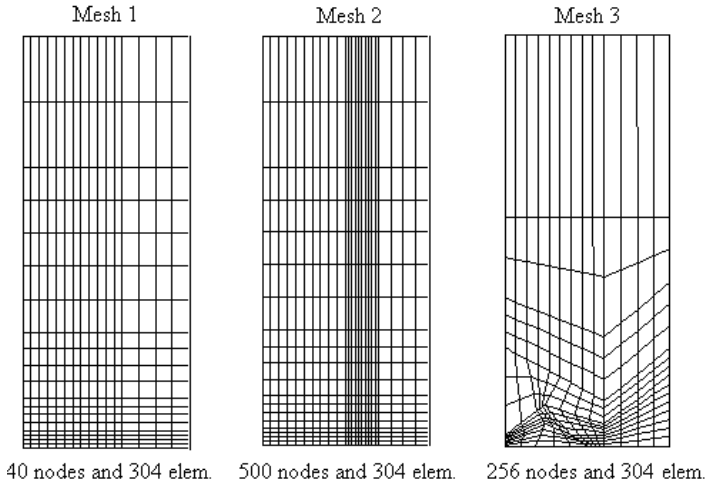

Figure 17: Double-edge-cracked plate – Different meshes considered.

transition between regions I and II where the material can no longer resist to mechanical solicitations. If a constant k=0.5 MPa.mm^2 is considered instead of k=1 MPa.mm^2, the fracture is more localized.

5 Conclusion

In the present paper it is proposed a framework, as simple as possible, to perform structural integrity analysis of quasi-brittle structures undergoing general loading (degradation due to the deformation process, crack initiation, crack propagation, total rupture) using a gradient-enhanced continuum dam-

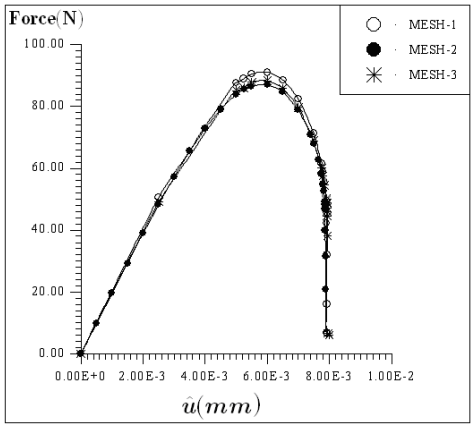

Figure 18: Double-edge-cracked plate. Tensile force versus displacement $\hat{u}$.

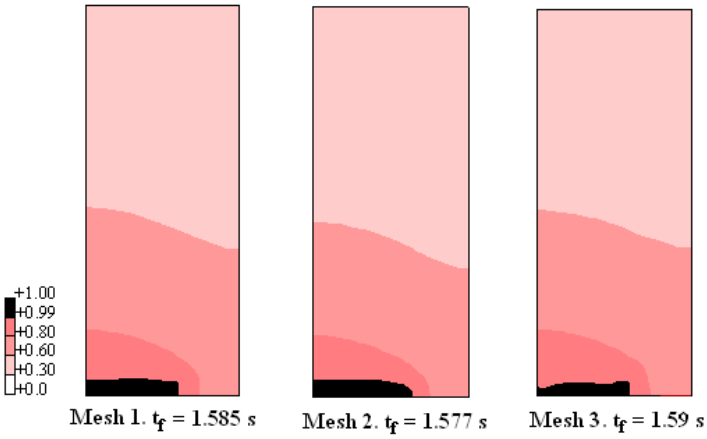

Figure 19: Double-edge-cracked plate. Damage distribution at the instant t_f when total failure occurs.

age model. A simple numerical technique was proposed to approximate the solution of the resulting nonlinear mathematical problem without the necessity of radical modification of an ordinary finite element code. The basic idea is to consider a splitting technique that transforms the global nonlinear problem in a sequence of linear problems that can be approximated using classical The basic idea is to consider a splitting technique that transforms the global nonlinear problem in a sequence of linear problems that can be approximated using classical discretization techniques. The Finite Element technique was adopted to obtain the semi-discrete problem. Nevertheless, the notation was kept intentionally general and abstract, since any adequate choice of base functions (such as in the element-free

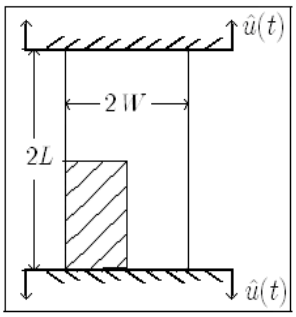

Figure 20: Clamped plate.

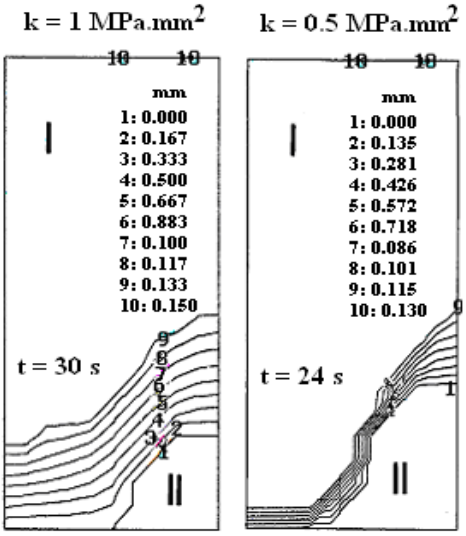

Figure 21: Clamped plate. Longitudinal displacement (mm) for two different values of k.

Galerkin method) can also be adopted alternatively in the semi-discretization. The numerical results are indiscernible within the precision of the figures if different time integration techniques (different values of θ) were adopted or different splitting techniques (section 3.2) were applied to the semi-discrete problem.

The theory allows a correct qualitative description of the strain-softening phenomena, is valid for any kind of geometry and for any kind of external loading, and can be seen as a first step towards a reasonably simple and practical tool to model the fracture of quasi-brittle structures(ceramics, concretes, rocks, glasses, etc.). Within this framework of microstructure theory, more sophisticated

boundary conditions for the damage variable can be considered to include adherence, for instance, through the external contact microscopic force.

References

[1] Lemaitre, J. & Chaboche, J.L., *Mechanics of Solids Materials*. Cambridge University Press, 1990.

[2] Knowles, J.K. & Sternberg, E., On the failure of ellipticity and the emergence of discontinuous deformation gradients in plane finite elastostatics. *J Elasticity*, **8**, pp. 329–379, 1978.

[3] Pietruszczak, S.T. & Mroz, Z., Finite element analysis of the deformation of strain-softening materials. *Int J Numer Meth Engng*, **17**, pp. 327–334, 1981.

[4] Needleman, A., Material rate dependence and mesh sensitivity in localization problems. *Comput Meth Appl Mech Engng*, **67**, pp. 69–87, 1988.

[5] Bazant, Z.P. & Pijaudier Cabot, G., Nonlocal continuum damage, localization, instability and convergence. *ASME J Appl Mech*, **55**, pp. 287–293, 1988.

[6] Bazant, Z.P. & Cedolin, L., *Stability of structures - elastic, inelastic and damage theories*. Oxford University Press, 1991.

[7] Costa-Mattos, H.S., N., M.E. & M., F., A simple model of the mechanical behavior of ceramic-like materials. *Int J Solid and Struct*, **24**, pp. 3185–3200, 1992.

[8] Frémond, M. & Nedjar, B., Damage, gradient of damage and principle of virtual power. *Int J Solids Structures*, **33(8)**, pp. 1083–1103, 1996.

[9] Khoei, A.R. & Karimi, K., An enriched-FEM model for simulation of localization phenomenon in cosserat continuum theory. *Comp Materials Science*, **44**, pp. 733–749, 2008.

[10] Peyrot, I., Bouchard, P.O., Bay, F., Bernard, F. & Garcia-Diaz, E., Numerical aspects of a problem with damage to simulate mechanical behavior of a quasi-brittle material. *Comp Materials Science*, **40**, pp. 327–340, 2007.

[11] Brighenti, R., A new discontinuous FE formulation for crack path prediction in brittle solids. *Int J Solid and Struct*, **45**, pp. 6501–6517, 2008.

[12] Lorentz, E., A mixed interface finite element for cohesive zone models. *Comput Methods Appl Mech Engrg*, **198**, pp. 302–317, 2008.

[13] Costa Mattos, H.S. & Sampaio, R., Analysis of the fracture of brittle elastic materials using a continuum damage model. *Struct Eng and Mechanics*, **3(5)**, pp. 411–427, 1995.

[14] Mindlin, R.D., Microstructure theories in linear elasticity. *Arch Rat Mech Anal*, **16**, pp. 51–78, 1964.

[15] Toupin, R.A., Theories of elasticity with couple-stress. *Arch Rat Mech Anal*, **17**, pp. 85–112, 1964.

[16] Armero, F. & Simo, J.C., A new unconditionally stable fractional step methods for non-linear coupled thermomechanical problems. *Int J Numerical Methods in Engineering*, **35**, pp. 737–766, 1992.

[17] Simo, J.C. & Miehe, C., Associative coupled thermoplasticity at finite strains: formulation, numerical analysis and implementation. *Comput Meth Appl Mech Engng*, **98**, pp. 41–104, 1992.

[18] Yanenko, N.N., *The Method of Fractional Steps*. Springer-Verlag: New York, 1980.

[19] Chorin, A.J., Hughes, T.J.R., McCracken, M.F. & Marsden, J.E., Product formula and numerical algorithms. *Communications on Pure and Applied Mathematics*, **31**, pp. 205–256, 1978.

[20] Belytschko, T., Lu, Y.Y. & Gu, L., Element free Galerkin methods. *Int J for Numerical Methods in Engineering*, **37**, pp. 229–256, 1994.